

Analysis on regional vegetation changes in dust and sandstorms source area: a case study of Naiman Banner in the Horqin sandy region of Northern China

Yun Zhou · Xueli Chang · Shengxing Ye ·
Zhirong Zheng · Shihai Lv

Received: 21 December 2013 / Accepted: 12 July 2014 / Published online: 13 August 2014
© Springer-Verlag Berlin Heidelberg 2014

Abstract Dust and sandstorms are disastrous meteorological processes in arid and semi-arid regions and are also an important indicator for evaluating desertification levels. The Horqin sandy region is an important transit zone and affected area of East Asian dust and sandstorms in Northern China. Over the past decades, the Chinese government has initiated several major ecological construction and sand-source control programs to effectively reduce and lessen the occurrence of dust and sandstorms. Taking Naiman Banner as an example, this paper evaluated the dynamics of vegetation restoration at Horqin sandy land using both field survey and remote sensing monitoring. Results showed a decreasing trend of shifting dunes from 1975 to 2008 and an increasing trend of connected fixed dunes at the desertification region in the north of the study area from 1985 to 2008 due to the large scale of eco-restoration programs. The increase of the vegetation remnants coverage in the non-growing seasons was consistent with the improvement of vegetation productivity in the

growing season, which could effectively help increase the topsoil's roughness in sandy land and ease soil wind erosion and desertification. In general, the regional vegetation environment maintained a benign circle. In particular, the effective vegetation restoration initiatives in the region will play a significant role in diminishing the occurrence of dust and sandstorms.

Keywords Vegetation restoration · Environmental changes · Production patterns · Non-growing seasons · Horqin sandy region

Introduction

The term dust and sandstorms denotes a disastrous meteorological process that occurs in arid and semi-arid regions that have occurred throughout the recent history and ancient geological time (Awadh 2012). It is also an important indicator for evaluating desertification levels at a given site (Ye et al. 2000; Song et al. 2005). Dust and sandstorms are a meteorological process (Goudie 1983; Littmann 1991; Pye 1987) and are triggered by strong airflow movement. The storms enact a large-scale transport process of fine particulate matters produced by surface wind erosion. Generally, there are three necessary conditions for dust and sandstorm development, namely strong wind, sufficient sand–dust source and unstable air stratification. More specifically, the necessary meteorological and thermal conditions include loose and dry dust on the earth's surface, the addition of strong and continual wind and unstable air stratification (Wang et al. 2001).

A large amount of research demonstrates that air current in the source area is responsible for the movement of dust

Y. Zhou
School of Environment, Beijing Normal University,
Beijing 100875, China

Y. Zhou · S. Ye · Z. Zheng · S. Lv (✉)
Chinese Research Academy of Environmental Sciences,
Beijing 100012, China
e-mail: 13801287270@163.com

X. Chang
Institute of Geography and Planning, Ludong University,
Shandong 264025, China

S. Ye
Key Laboratory of Soil and Water Conservation and
Desertification Combating, Ministry of Education, School of Soil
and Water Conservation, Beijing Forestry University,
Beijing 100083, China

and sand particles, but the turbulent fluctuation of air current with dust particles is mainly affected by the features of the underlying surface (Judd et al. 1996). McTainsh et al. argue that the meteorological conditions for dust and sandstorms are primarily related to soil moisture and vegetation conditions, and then wind (McTainsh 1998; Miller et al. 2004). Yang's research (2010) shows the correlation between the occurrence frequencies of floating dust with the wind speed, temperature and transpiration rate in the Shapotou region of North China, and the reduction of the surface average relative humidity aggravates the frequency of floating dust weather. In the formation process of a dust and sandstorm, dust-released flux is proportional to the surface soil saltation flux, while the surface soil saltation flux is closely linked to the underlying surface types (Alfaro and Gomes 2001; Liao and Seinfeld 1998). The study of Zhao et al. (2011) shows that the transportation of sand–dust at the desert and edge of oasis sites mainly occurs in the near-ground layer, while at the oasis site, the transportation is mainly concentrated in the upper layer. Their research also indicated that vegetation, especially the windbreak shelterbelt, plays an important role in reducing sand–dust flux; for example, compared with the desert site, the edge of the oasis site has 42.0 % less sand–dust and the oasis site has 74.4 % less. The different features of the underlying surface in each region impact the intensity of the storms. Iwasaka (1983) argues that at the regional scale, land use, land cover condition and productivity level within growing seasons and vegetation remnants coverage in the non-growing seasons also exert significant influence on the dust and sandstorm process.

In natural grasslands, the increasing vegetation coverage can increase the surface roughness, which lessens the occurrence of dust and sandstorms. Observation shows that vegetation coverage between 15 and 25 % on sandy soil reduces ground wind erosion by 21–31 % of bare, shifting dunes. In contrast, wind erosion accounts for only 0.95 % of the shifting dunes when vegetation coverage reaches 40–50 %, demonstrating why grassland with high vegetation coverage is not likely to produce dust and sandstorms. Additionally, the thick roots of vegetation can consolidate soil, so they are susceptible to wind erosion. Vegetation adapted to shifting sand could reverse the desertification process and reduce the occurrence of dust and sandstorms (Roels et al. 2001). In sandy regions, particularly areas with shifting sand, low vegetation coverage and low roughness decreases the start wind speed of soil erosion and increases soil saltation flux and dust transport quantity. In addition, the composition of eolian sandy soil also heavily impacts dust and sandstorm occurrence. When the wind speed is certain, the quantity of fugitive dust depends on the amount of dust, sand and clay particles (<0.063 mm) in the surface

soil, while the eolian fine sand with a high content of soil-erodible particles such as fine silt and clay can provide plenty of sand–dust sources for dust and sandstorm occurrence (Mei et al. 2004a, b).

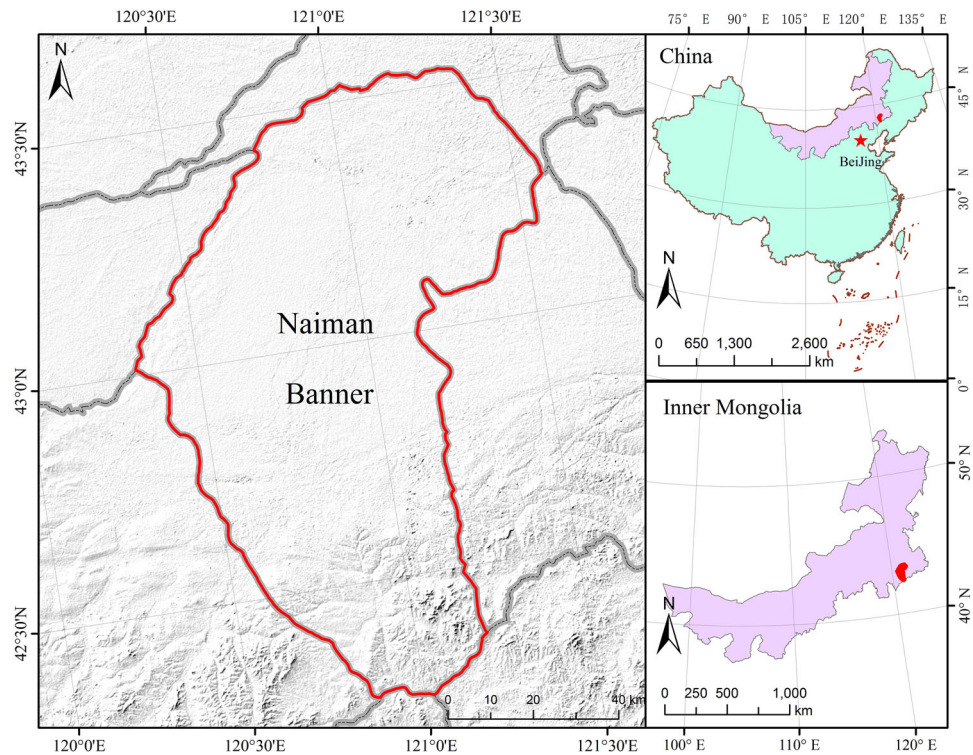
In the arid and semi-arid regions of Northern China, there are three major dust and sandstorm invasion paths (Zhu and Zheng 2002). The first path is the north path, originating from the desert–steppe area of Southeast Mongolia (source region), and passing through Ulanchoabu, Xinlin Gol, Chifeng and Tongliao in Inner Mongolia to the center of North China, Beijing, Tianjin, Tangshan and the southern part of Northeast China. The second path is the northwest path, originating from the desert and desert–steppe at the central southern part of Mongolia (source region), and passing through the Alxa League, Hexi Corridor, Maowusu Sandy Land, Ulan Buh Desert, Hohhot in Inner Mongolia, Zhangjiakou and then to Beijing, Tianjin and Tangshan. The third path is the west path, originating from the edge of Taklimakan Desert at Tarim Basin (source region) and passing through Dunhuang, Jiuquan, Zhangye, Minqin, Yanchi, Etoke Banner and Datong, to Beijing, Tianjin and Tangshan. The Horqin region is located at the north path. This paper analyzed the changes in land use and coverage in recent decades within the typical regions of Horqin and evaluated the role of Horqin sandy land in dust and sandstorm development in this region, providing the foundation for dust and sandstorm pre-warning and control.

Study area

Naiman Banner is located in the east of Inner Mongolia Autonomous Region, and the south edge of the Horqin sandy region in the east farming–pastoral ecotone of the arid and semi-arid areas in Northern China with a total area of 8,120 km² (E120°19'40"–121°35'40", N42°14'10"–43°32'20") (Fig. 1). The geomorphology changes from tectonic mountains to alluvial wavy plain and alluvial valley plain. The topography is high in the south and low in the north. The south comprises low hills and a cinnamon soil platform with an average altitude of 400–500 m and is situated at the longitudinal tectonic belt of the Yinshan Mountains and the uplift belt of New Cathaysian System's third system. The central area is alternated with sand bog and dunes with an altitude of 300–400 m. The main landscape comprises fixed dune, semi-fixed dune, shifting dune and marshy grassland, which are distributed alternatively. In the north is the Kailu Basin in the twisted and Songliao compressed tectonic belt. At this location, the land is flat with fertile soil with an average altitude below 300 m.

Naiman Banner falls within temperate continental and semi-arid climate zones with average temperatures of

Fig. 1 Location of Naiman Banner



6.8 °C and annual precipitation of 366.3 mm. Rainfall is mainly concentrated in June, July and August, accounting for 67.4 % of the annual precipitation. The annual evaporation is 1,935 mm, which is 5.3 times the average precipitation. The days over 8 grade wind are 33.5 days per annum, occurring mainly in spring (from March to May) and accounting for 55–61 % of the annual total days. The annual average days with dust and sandstorms are 7.6 days, while the maximum reaches 23 days.

The soil can be categorized into five types, namely cinnamon soil, chestnut soil, meadow soil, eolian sandy soil and bog soil. Cinnamon soil is distributed at the south, accounting for 16 % of the total area; chestnut soil is generally dispersed at the central south covering 65 % of the total area, most of which has already developed into eolian sandy soil with coarse texture and loose structure; while the meadow soil and bog soil are concentrated along the rivers, sand bogs, lakes and other lowlands. Due to intense human interference, zonal vegetation in this region becomes secondary vegetation to a large extent. In most parts, zonal vegetation has been replaced by semi-recessive vegetation such as sand, shrub and recessive meadow vegetations. The main plant species in this region are shrub, perennial herbaceous plants and annual herbaceous plants including *caragana microphylla*, *artemisia halodendron*, *artemisia frigida*, *mellissitus ruthenicus*, *cleistogenes squarrosa* and *setaria viridis*.

Method

Collection of land use/land cover information

Field investigation was combined with the visual interpretation of two MSS images (1975 and 1985) and three Landsat TM images (1995, 2005 and 2008). ERDA’s Erdas8.6 software was adopted to undertake geometric calibration and projection transformation to achieve accurate spatial registration of images. The research methodology used in this paper is shown in Fig. 2. Images interpretation and topology was completed by ArcGis9.1 with display accuracy of the interpretation screen between 1: 50,000 and 1:100,000. According to the features of the landscape reflected from the images and actual conditions of Naiman Banner, the northern region of Naiman Banner is selected as the study area and is categorized into four types of sandy land based on Zhu’s sandy land division principle (1981): shifting dunes, semi-shifting dunes, semi-fixed dunes and fixed dunes.

Collection of land productivity information

Analysis on the regional productivity was based on the 16-day synthetic NDVI data of EOS-Modis/Terra provided by American USGS to global customers free of charge with a resolution of 250 m. A data time frame of 11 years was

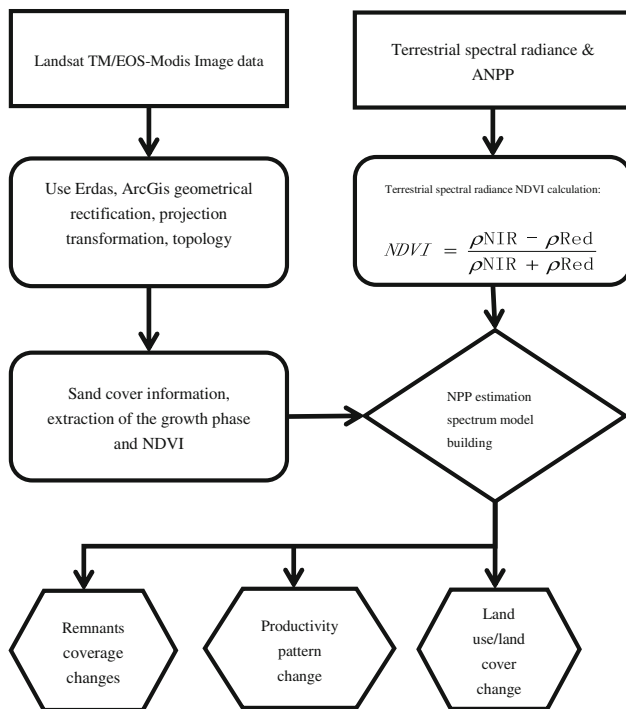


Fig. 2 Research methodology

selected (2000–2010) and acquired on June 26th. Image calibrations were completed based on the TM images in the same region.

Determination of ground spectrum and annual aboveground net primary productivity (ANPP)

Spectrometric determination of meadow vegetation was undertaken from June 18 to 20, 2011 using American ASD Company's FieldSpec 1 spectroradiometer. In the process, the sensor was set vertically and 0.5 m from the canopy, and a standard light calibration board was used every 10–15 min. This work was conducted under sunny day with clear, low wind, as well as intense and stable sunlight. The field spectrometric determination time ran between 10:00 am and 3:00 pm.

Five groups of spectral data were collected from each quadrant. Plants were neatly cut along the ground. After fresh weight was weighed, they were put in cloth bags and taken back to dry at 80 °C constant temperature for 10–12 h and then the dry weight was determined. Since NPP included the underground growth increment and the amount eaten by herbivores, it was impossible to obtain entirely accurate data. Therefore, NPP in this paper was replaced by ANPP (Tilman 1996, 2001).

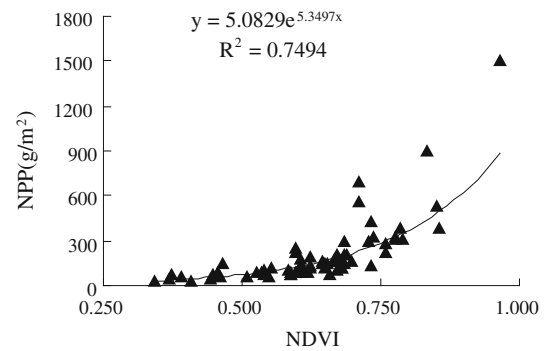


Fig. 3 Spectrum model of aboveground biomass in June in Naiman Banner

NDVI calculation of ground spectrum

ASD's ViewSpec pro software (version 5.6) was used to process the obtained ground spectral data to determine the average spectral reflectivity of the red spectral band (0.62–0.67 μm) and near-infrared waveband (0.841–0.876 μm) which were consistent with the Modis satellite waveband. The NDVI calculation formula was as follows:

$$\text{NDVI} = (\rho_{\text{NIR}} - \rho_{\text{Red}}) / (\rho_{\text{NIR}} + \rho_{\text{Red}}) \quad (1)$$

where ρ_{NIR} and ρ_{Red} are the average spectral reflectivity of the near-infrared waveband and red spectral band, corresponding to Modis satellite data.

Construction of NPP estimation spectrum model

Estimation of the aboveground dry matter quantity from ground spectrum model was established based on the correlation analysis of NDVI and aboveground biomass of current year from the collected ground spectral data.

Existing research showed that there were internal links between the actual measured and monitored ground vegetation spectral features by remote sensing. The actual measured ground vegetation spectral features can be used to replace the monitored ground vegetation spectral features by remote sensing (Li et al. 2001; Xu 2008). 68 groups of data were used to develop a high spectrum ANPP Model in Naiman Banner (Fig. 3):

$$y = 5.0829e^{5.3497x} \quad (2)$$

where y represented NPP of the current year with a unit of g/m^2 ; x represented NDVI value, and the test of significance of correlation coefficient reached the most significant level ($R = 0.8639 > R_{0.01,67} = 0.1480$). According to formula (2), the NDVI data were calculated using grid calculation function in the spatial analyst module of Arcgis to produce 250×250 m productivity structure maps.

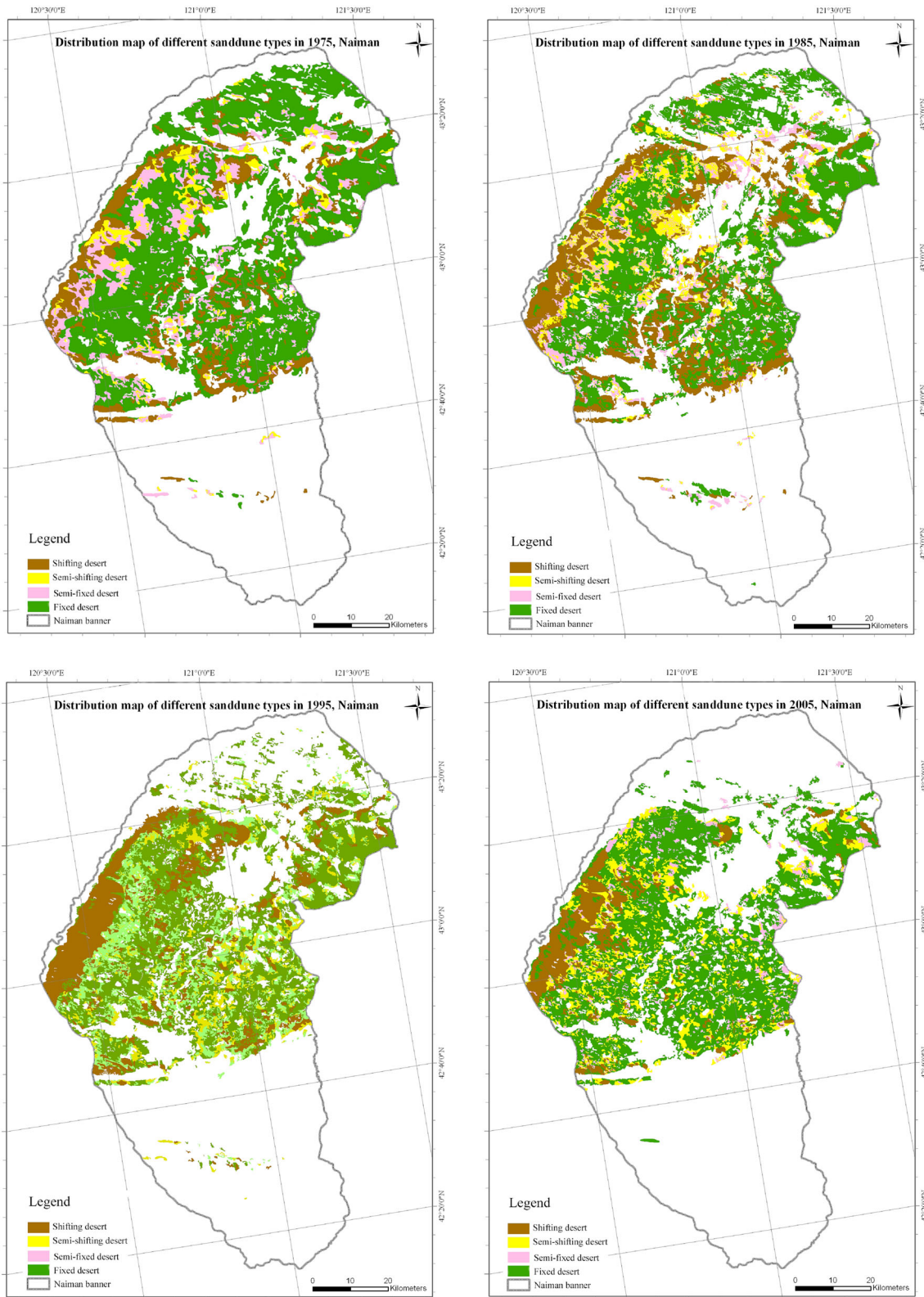


Fig. 4 The distribution map of different sand dunes in Naiman Banner

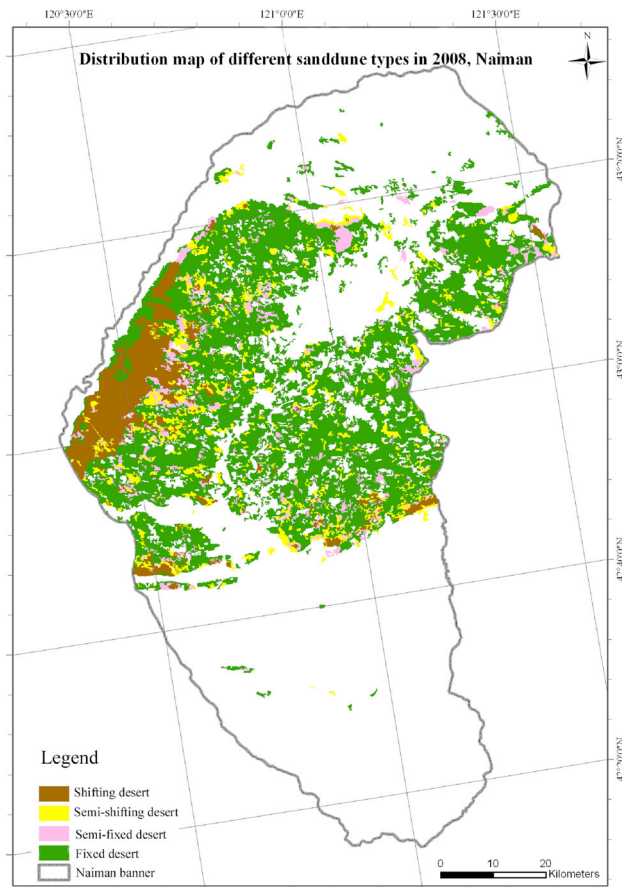


Fig. 4 continued

Collection of vegetation coverage in the non-growing seasons in sandy land

Landsat TM data from 1989, 1995, 2000 and 2007 were collected to get the information about vegetation coverage in non-growing seasons in sandy land. Given that waveband 3 (0.62–0.69) of Landsat TM data was the optimal waveband of visible light for extracting information of vegetation, lithology, strata, structure and geomorphology and sensitive to sand–dust and vegetation chlorophyll, the research applied TM data at the non-growing seasons as the data source to conduct bare surface extraction within the largest dune (including all kinds of dunes) region (1975) for interpreting land use cover.

The construction of bare surface extraction model was completed by the Model Maker module of Erdas9.1. This module had key algorithmic language and programming, which can establish the logical and conditional statement of model calculation through this language, and export image data translated by pixel grayscale value of bare land (Valuation 1) and with vegetation cover (Valuation 0). The circle demonstrated the model's operational set, which was composed of logical language and

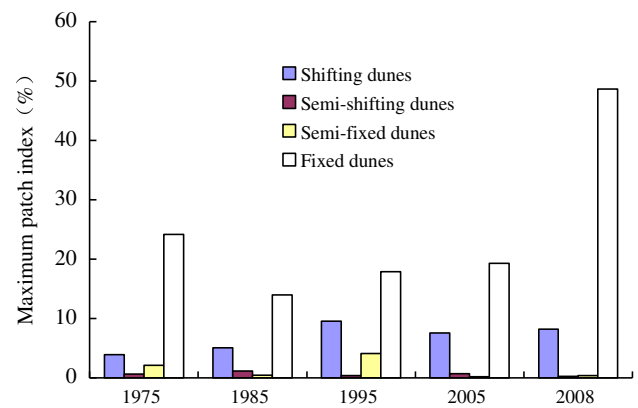


Fig. 5 Changes in maximum patch index of different types of dunes

Table 1 Change in the features of different types of dunes (hectare)

Year	Shifting dunes	Semi-shifting dunes	Semi-fixed dunes	Fixed dunes	Total
1975	69,006	25,520	62,737	262,298	419,561
1985	97,445	43,876	45,424	207,236	393,981
1995	74,861	33,916	64,612	184,420	357,808
2005	44,398	54,887	20,074	210,495	329,854
2008	36,107	35,900	24,226	214,678	310,911
Average	64,363	38,820	43,415	215,825	

computational language, while the arrows represented the calculation procedure.

Results

Land use and land cover changes in sandy regions

In the past 30 years, strong increase in greenness was observed over large areas of the Northern China from the NDVI data (An et al. 2013; Duan et al. 2011), demonstrating that the reduction was mainly due to the conversion from sandy land to farm land and forest land. Our result showed that the acreage of sandy land had decreased to 1086.50 km² from 1975 to 2008 with an average annual decrease of 32.92 km² (Fig. 4; Table 1). In terms of the general features of the 5 years, the distribution acreage of fixed dunes and shifting dunes were comparatively large (2,158.25 and 643.63 km², respectively), while semi-fixed dunes and semi-shifting dunes were comparatively small (388.20 and 434.15 km², respectively).

Second, we examine the changing features of different types of dunes. The acreage of fixed dunes had grown smaller from 1975 to 1995 and then began to increase following that year. The trend of shifting dunes had

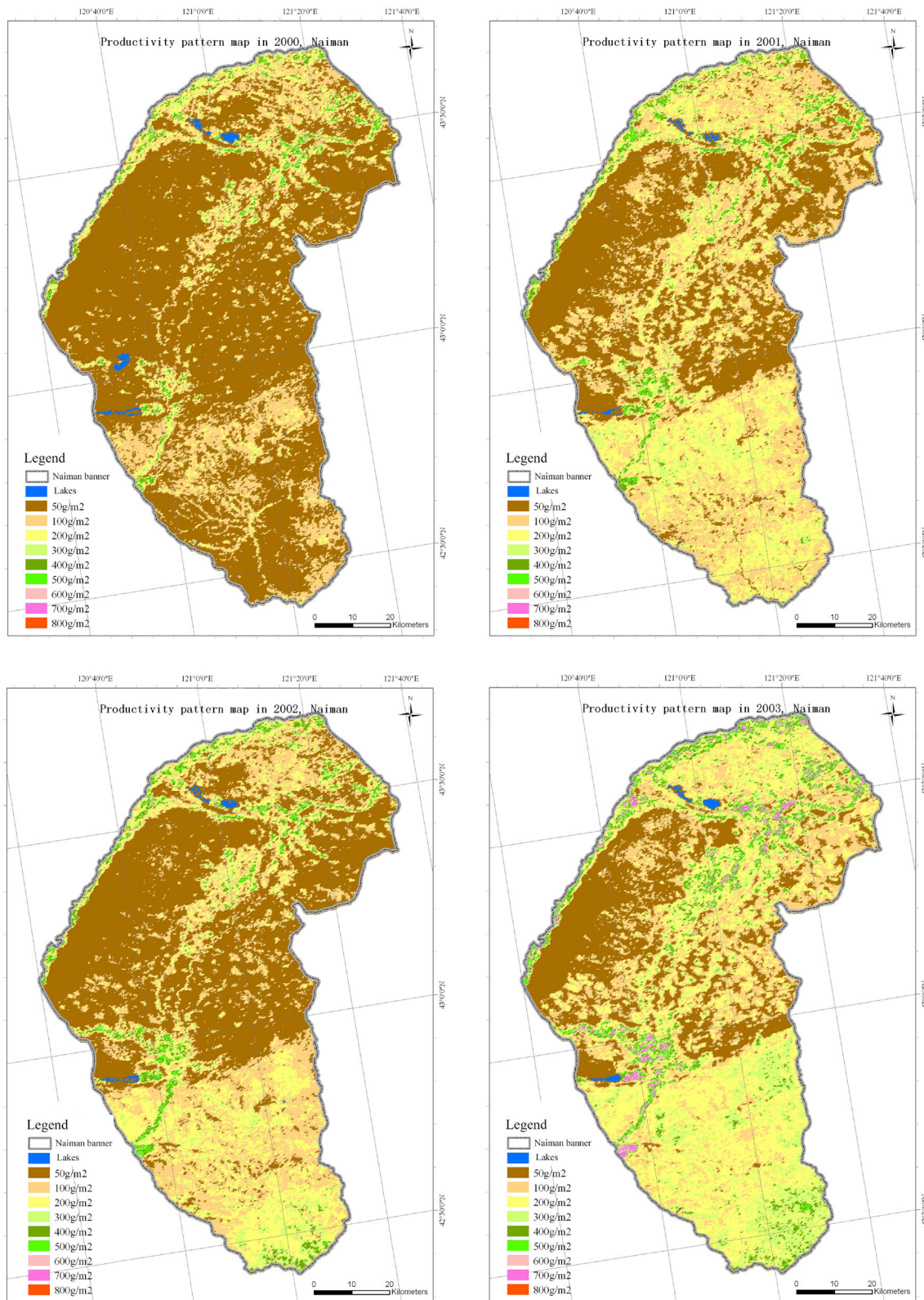


Fig. 6 Distribution map of productivity patterns at different times in Naiman Banner

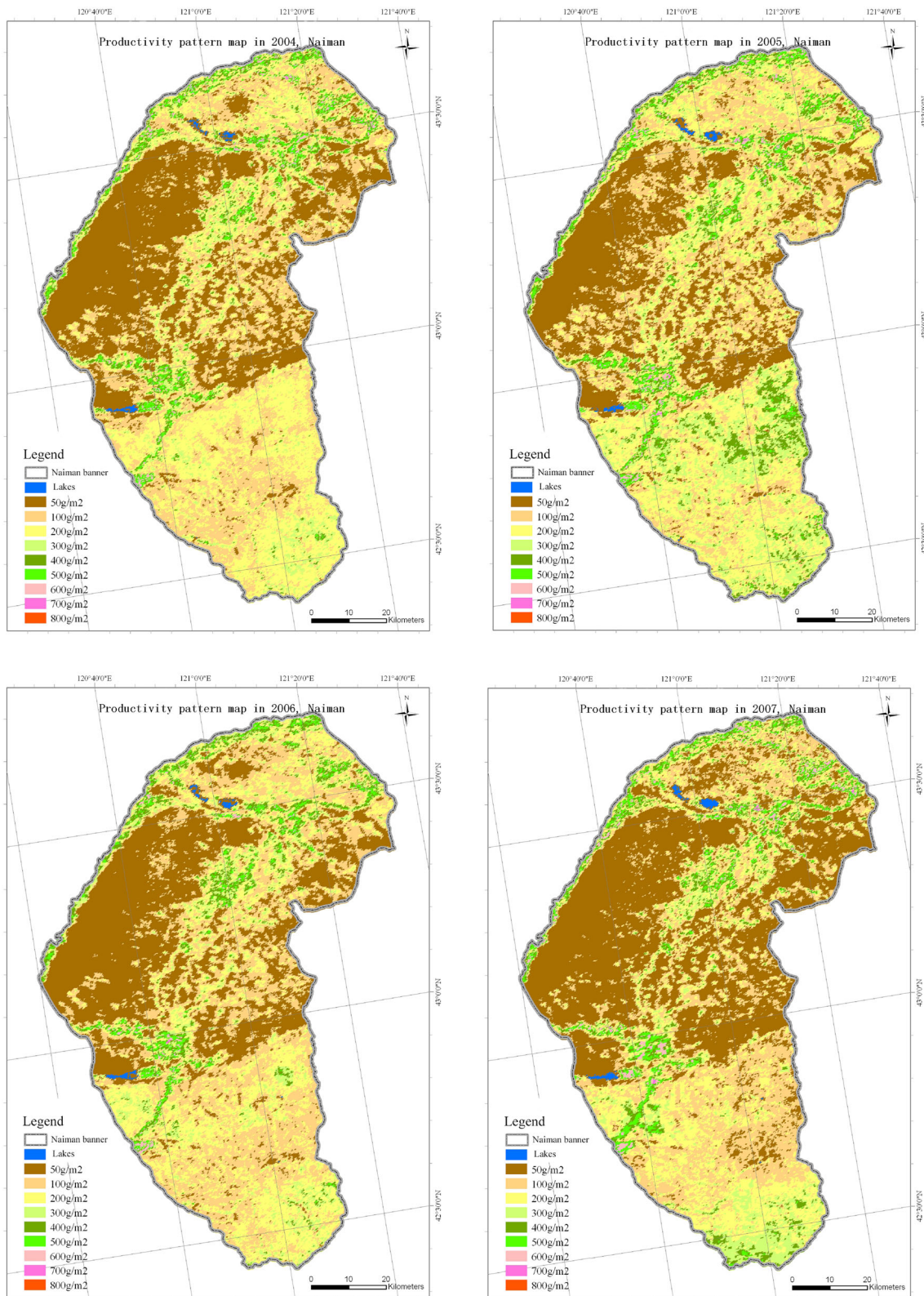


Fig. 6 continued

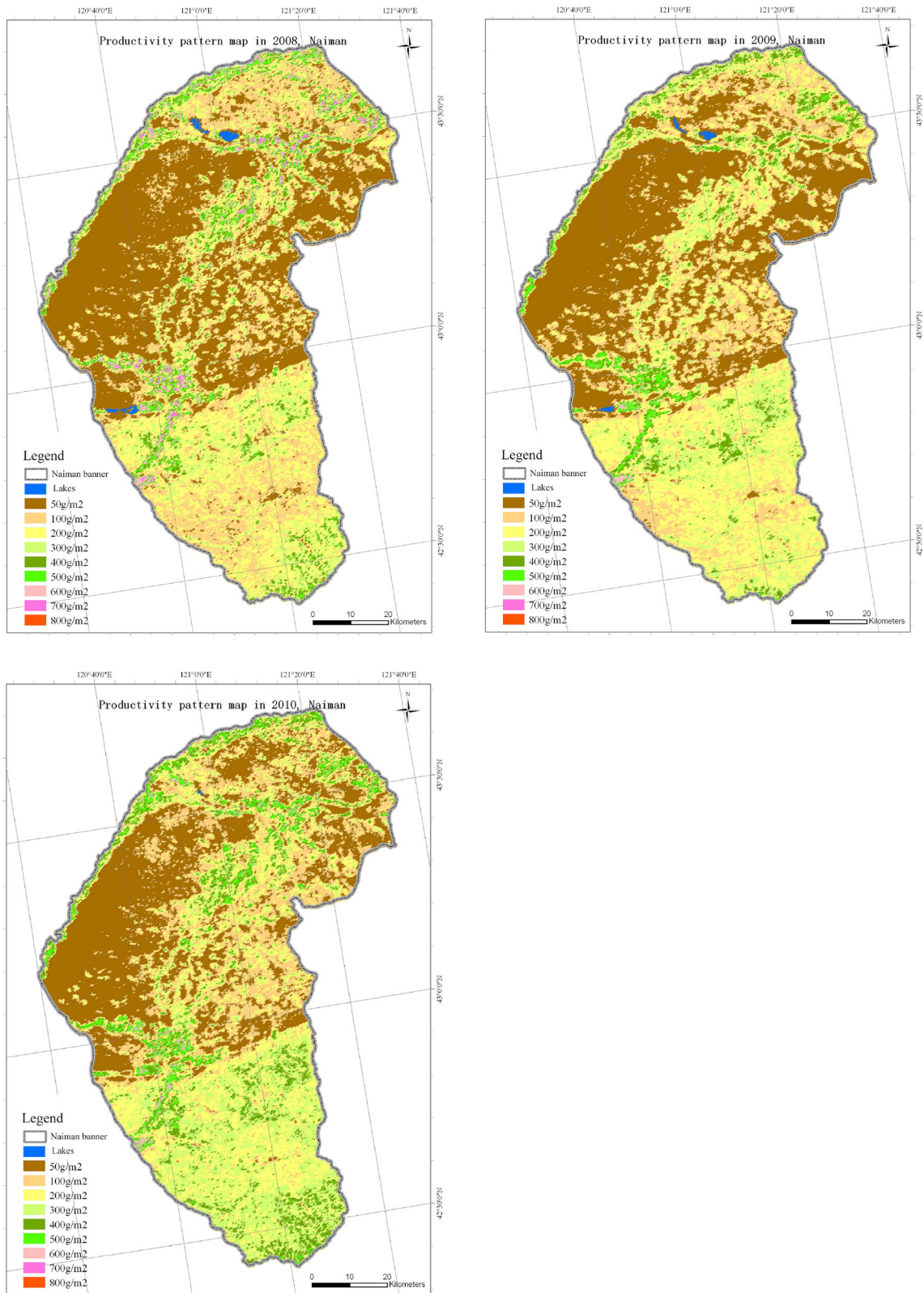


Fig. 6 continued

Table 2 Acreage distribution features of different productivity capacities (hectare)

	Year										
	2000	2001	2002	2003	2004	2005	2006	2007	2008	2009	2010
Water body or bare land (g/m^2)	3,334	1,518	1,899	2,151	1,498	1,767	1,739	2,307	2,386	1,408	101
<50	546,844	270,740	374,507	180,864	254,611	196,120	258,912	324,227	290,003	278,551	232,891
50–100	177,253	268,611	214,575	186,948	231,900	196,683	249,562	203,898	197,387	168,556	161,009
100–200	58,438	210,255	157,259	275,865	225,250	234,970	195,790	154,714	179,298	220,764	189,310
200–300	19,855	44,656	41,878	103,230	55,451	109,056	60,581	66,432	73,985	101,065	146,588
300–400	10,250	18,165	19,972	34,700	27,620	52,021	33,944	36,952	35,083	37,449	61,193
400–500	4,783	7,369	10,087	18,737	19,775	23,805	17,688	24,113	23,377	11,937	25,569
500–600	1,021	417	1,591	13,593	5,568	7,174	3,488	8,816	17,285	2,037	5,115
600–700		41	8	5,632	103	180	61	319	2,973	10	
700–800				57							
Total productivity (t)	469,958	795,465	719,240	1,174,863	931,033	1,151,462	915,016	920,526	1,016,825	975,919	1,186,783

increased from 1975 to 1985, and started to decrease since then. The changes in semi-fixed and semi-shifting dunes were comparatively complicated. The acreage of semi-fixed dunes became the biggest in 1995 and the smallest in 2005, while that of semi-shifting dunes was the biggest in 2005 and the smallest in 1975.

Third, we observed the changing features of the maximum patch index. Specifically, we examined the single maximum patch as it accounted for the total acreage of all types of patches (Fig. 5). The maximum index of fixed dunes was the largest of all types with the highest of 48.7 % in 2008 and the lowest 14.0 % in 1985, followed by shifting dunes that reached the highest of 9.5 % in 1995 and the lowest of 3.9 % in 1975. The maximum patch index of semi-fixed and semi-shifting dunes was comparatively small and never surpassed 5 % at their highest levels.

Changes in productivity pattern

Based on the spectrum-biomass model and ArcGis spatial analysis and mapping calculation, the productivity pattern map, the corresponding spatial distribution data from 2000 to 2010 and regional productivity capacity calculated with mean values were obtained (Fig. 6; Table 2).

From the analysis in Table 2, the acreage of productivity capacity per unit less than $50 \text{ g}/\text{m}^2$ decreased with fluctuation each year. The actual acreage gradually decreased from $5,468.44 \text{ km}^2$ in 2000 to $2,328.91 \text{ km}^2$ in 2010 with an average annual decrease of 285.41 km^2 .

On the contrary, acreage had increased gradually from $584.38, 198.55, 102.50$ and 47.83 km^2 in 2000 to $1,893.10, 1,465.88, 611.93$ and 255.69 km^2 in 2010, respectively, in

areas with the productivity capacity per unit of 100–200, 200–300, 300–400 and $400\text{--}500 \text{ g}/\text{m}^2$.

The change of total productivity capacity had increased gradually from $469,958 \text{ t}$ in 2000 to $1,186,783 \text{ t}$ in 2010.

Changes in vegetation remnants coverage in the non-growing seasons in the sandy region

Naiman Banner is located in the farming–pastoral ecotone of the arid and semi-arid areas in North China. This area suffers severe soil erosion and frequent dust and sandstorms due to climate change and human interference. Storms most frequently occur in the dry winter and spring. The most likely factors that influence the occurrence of dust and sandstorms are the features of underlying surface and vegetation remnants coverage in the non-growing seasons (Sun et al. 2001; Zhou and Wang 2002). The analysis of remote sensing showed that vegetation remnants coverage in the non-growing seasons had increased from 1989 to 2007 (Fig. 7). In terms of the changes in vegetation remnants coverage in sandy land, the acreage had grown from $2,686.76 \text{ km}^2$ in 1989 to $3,250.39 \text{ km}^2$ in 2007 with an increase of 563.63 km^2 . The changes in the maximum patch index of vegetation remnants covered area were consistent with the acreage change trend, which was 56.5 % in 1989 and 75.8 % in 2007 with an augmentation of 19.3 %.

Conclusion

At the desertification region in the north of the study area, there existed the largest acreage distribution of fixed dunes and shifting dunes, in which the acreage decrease of

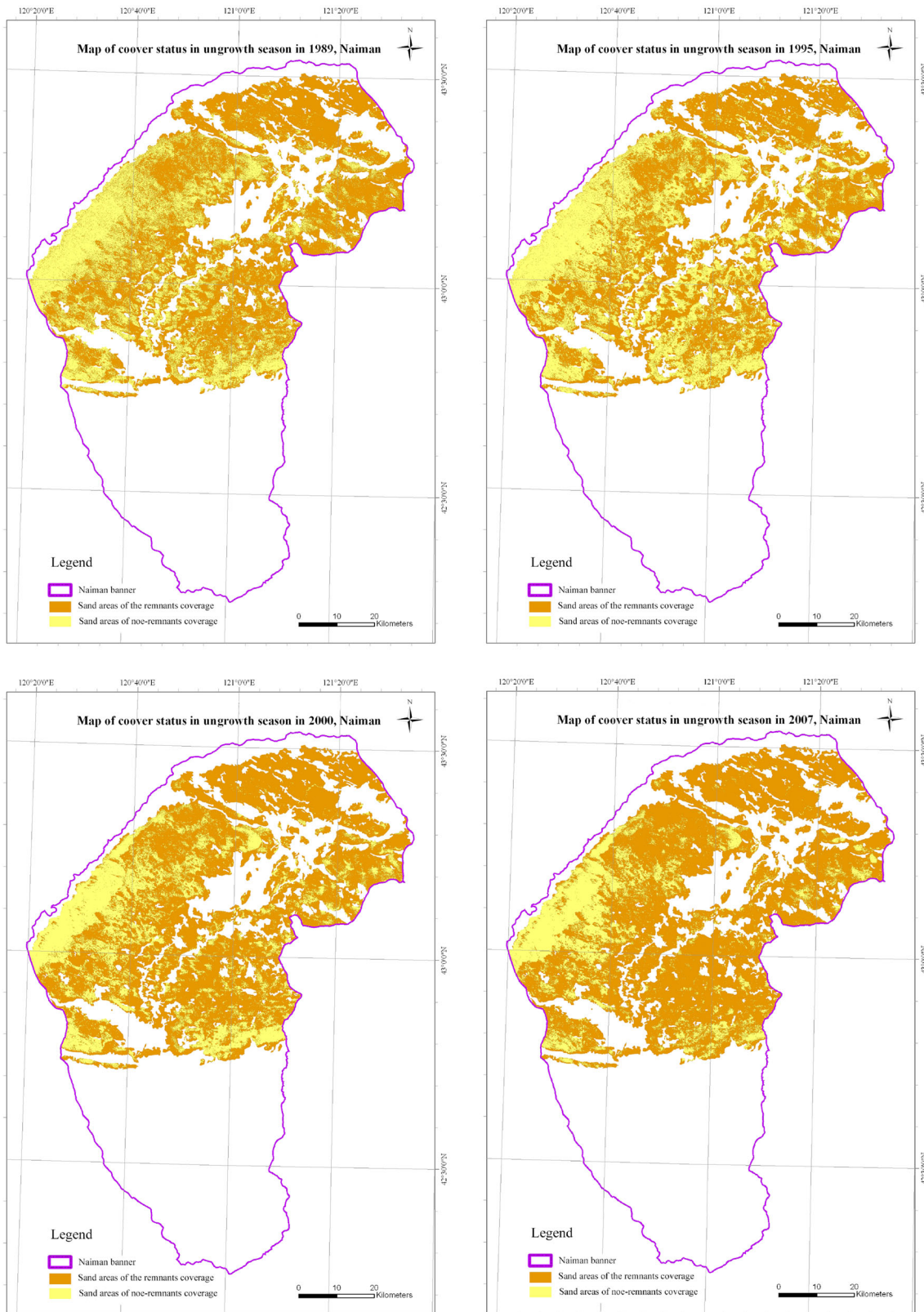


Fig. 7 Coverage changes in vegetation remnants in the non-growing season

shifting dunes and the increase of maximum patch index of fixed dunes became the most remarkable characteristics of land use and land cover change. Shifting dunes had decreased 328.99 km² from 1975 to 2008 with an average annual reduction of 9.97 km², while the maximum patch index of fixed dunes had increased from the lowest 13.97 % in 1985 to 48.67 % in 2008. This demonstrated that the vegetation area in the north sandy region was characterized by reduced shifting dunes and increased connected fixed dunes. These changes might be directly linked to the large-scale eco-restoration programs, which had been focusing on desertification land control, conversion of farmland to forest and grassland and re-plantation in the Horqin region since 2002. From the perspective of the productivity pattern changes within the growing season (June), the acreage of low-productivity regions (<50 g/m²) had decreased from 5,468.44 km² in 2000 to 2,328.91 km² in 2010 with an average annual reduction of 285.41 km². Meanwhile, the acreage of the productivity level of 200–300 g/m² had increased from 198.55 km² in 2000 to 1,465.88 km² in 2010, with an average annual increase of 115.21 km². The regional vegetation productivity had grown from 469,958 t in 2000 to 1,186,783 t in 2010 with an average annual increase of 13.9 %. This showed that the vegetation in the Horqin region had improved significantly due to decades of efforts in eco-construction and restoration. In terms of the vegetation remnants coverage changes in the non-growing seasons in Horqin sandy regions from 1989 to 2007, the accumulative total acreage had increased by 563.63 km² with an average growth of 31.31 km². This was linked directly to the increase of vegetation coverage in the growing seasons in the designated region. The increase of the vegetation remnants coverage in the non-growing seasons could effectively increase the topsoil's roughness in sandy land and ease soil wind erosion and desertification, which in turn played an important role in lessening the occurrence and development of dust and sandstorms in the designated region (Iwasaka et al. 1983; Gu et al. 2002).

As the transit zone of the east pathway of dust and sandstorms in North China (Zhu and Zheng 2002), the regional vegetation environment in the Horqin sandy region maintained a benign cycle in the past decade in terms of the changes in land cover, vegetation features in the growing seasons and the remnants features of surface vegetation in the non-growing seasons. In particular, the effective vegetation restoration of the sandy region will play a significant role in lessening the frequency of dust and sandstorms in the Horqin region.

Acknowledgments This research work was funded by the China National Public Welfare Projects of Environmental Protection (201109025). Part of this research was based on the Joint Research on

Dust and Sandstorms-Working Group II: "Prevention and Control of Dust and Sandstorms" launched in 2007 by Tripartite Environment Ministers Meeting among China, Korea and Japan. The authors would like to thank the Ministry of Environmental Protection of China, the Ministry of the Environment of Japan and Korea Forest Research Institute for their contributions and support to this study.

References

- Alfaro SC, Gomes L (2001) Modeling mineral aerosol production by wind erosion: emission intensities and aerosol size distribution in source areas. *J Geophys Res* 106(16):18075–18084
- An YZ, Gao W, Gao ZQ (2013) Characterizing land condition variability in Northern China from 1982 to 2011. *Environ Earth Sci*. doi:10.1007/s12665-013-2987-6
- Awadh SM (2012) Geochemistry and mineralogical composition of the airborne particles of sand dunes and dust storms settled in Iraq and their environmental impacts. *Environ Earth Sci* 66:2247–2256
- Duan HC, Yan CZ, Tsunekawa A, Song X, Li S, Xie JL (2011) Assessing vegetation dynamics in the Three-North Shelter Forest region of China using AVHRR NDVI data. *Environ Earth Sci* 64:1011–1020
- Goudie A (1983) Dust storms in space and time. *Prog Phys Geogr* 7:502–530
- Gu W, Cai XP, Xie F, Li ZJ, Wu XH (2002) Study on the relationship between vegetation cover and distribution of days sand dust-storm occurrence—taking central western Inner Mongolia for example. *Adv Earth Sci* 17(2):273–277
- Iwasaka Y, Minoura H, Nagaya K (1983) The transport and special scale of Asian dust-storm clouds: a case study of the dust-storm event of April 1979. *Tellus* 35B:189–196
- Li C, Zhuang Y, Cao M, Crill P, Dai Z, Frohling S, Wang X (2001) Comparing a process-based agro-ecosystem model to the IPCC methodology for developing a national inventory of N₂O emissions from arable lands in China. *Nutri Cycl Agroecosystems* 60(1–3):159–175
- Judd MJ, Raupach, Fininigan JJ (1996) A wind tunnel study of turbulent flow around single and multiple windbreaks. part I: velocity and boundary layer. *Meteorology* 80(1/2):127–165
- Liao H, Seinfeld JH (1998) Radiative forcing by mineral dust aerosols: sensitivity to key variables. *J Geophys Res* 103(D24):31637–31645
- Littmann T (1991) Dust storm frequency in Asia: climatic control and variability. *Int J Climatol* 11:393–412
- McTainsh GH (1998) Climatic controls upon dust storm occurrence in eastern Australia. *J Arid Environ* 39(3):457–466
- Mei FM, Zhang XY, Lu HY, Shen ZX, Wang YQ (2004a) The impact of the micro particle groups' size distribution of the topsoil on dust release flux in north China. *Chin Sci Bull* 49(17):1776–1784
- Mei FM, Zhang XY, Cao JJ, Lu HY, Wang YQ (2004b) Quantitative assessment of the impact of vegetation cover category at the sand-dust source in north China on the intensity of topsoil wind erosion. *Mar Geol Qua Tern Geol* 24(1):119–124
- Miller RL, Tegen I, Perlwitz J (2004) Surface radiative forcing by soil dust aerosols and hydrologic cycle. *J Geophys Res* 109(D4):1–24
- Pye K (1987) Aeolian dust and dust deposits. Academic Press, London
- Roels B, Sebastiaan D, Marinus J, Erger AW (2001) Relation of wind-induced sand displacement to plant biomass and plant sand-binding capacity. *Acta Bot Sin* 43(9):979–982
- Song Y, Liu LY, Yan P, Cao T (2005) Influence of five types underlying surface on sand-dust storm in Northern China. *J Soil Water Conserv* 19(6):015–018

- Sun JM, Zhang MY, Liu TS (2001) Spatial and temporal characteristics of dust storms in China and its surrounding regions, 1960–1999: relations to source area and climate. *J Geophys Res* 106:10325–10333
- Tilman D (1996) Biodiversity: population versus ecosystem stability. *Ecology* 77(2):350–363
- Tilman D, Fargione J, Wolff B, D’Antonio C, Dobson A, Howarth R, Swackhamer D (2001) Forecasting agriculturally driven global environmental change. *Science* 292(5515):281–284
- Wang T, Chen GT, Qian ZA, Yang GS, Qu JJ, Li DL (2001) Current situation and countermeasure to the sand dust storm in north China. *J Desert Res* 21(4):322–327
- Xu JX (2008) High-frequency zones and abrupt changes of sandstorms in Loess Plateau Region of China. *J Desert Res* 1:025
- Yang FM, Chongyi E (2010) Correlation analysis between sand-dust events and meteorological factors in Shapotou, Northern China. *Environ Earth Sci* 59:1359–1365
- Ye DZ, Niu JF, Lin JY, Wang YM, Zhou Z, Ju HB, Huang HQ (2000) Causes of sand-stormy weather in Northern China and Control measures. *Acta Geogr Sin* 55(5):513–521
- Zhao M, Zhan KJ, Qiu GY, Fang ET, Yang ZH, Zhang YC, Li AD (2011) Experimental investigation of the height profile of sand-dust fluxes in the 0–50-m layer and the effects of vegetation on dust reduction. *Environ Earth Sci* 62:403–410
- Zhou ZJ, Wang XW (2002) Analysis of the severe group dust storms in eastern part of Northwest China. *J Geogr Sci* 12(3):357–362
- Zhu FK, Zheng XJ (2002) Southern boundary of dust storm in China. The first international workshop on sandstorm and associated dust fall (programme and abstracts), Seoul, Korea, pp 1–6